Published in final edited form as:
Bone. 2010 January ; 46(1): 18. doi:10.1016/j.bone.2009.10.025.

Transient muscle paralysis disrupts bone homeostasis by rapid degradation of bone morphology

Sandra L. Poliachik, **Steven D. Bain**, **DeWayne Threet**, **Philippe Huber**, and **Ted S. Gross**
Department of Orthopaedics and Sports Medicine University of Washington, Seattle, WA, 98104

Abstract

We have previously shown that transient paralysis of murine hindlimb muscles causes profound degradation of both trabecular and cortical bone in the adjacent skeleton within 3 weeks. Morphologically, the acute loss of bone tissue appeared to arise primarily due to osteoclastic bone resorption. Given that the loss of muscle function in this model is transient, we speculated that the stimulus for osteoclastic activation would be rapid and morphologic evidence of bone resorption would appear before 21 d. We therefore utilized high-resolution *in vivo* serial micro-CT to assess longitudinal alterations in lower hindlimb muscle volume, proximal tibia trabecular and tibia middiaphysis cortical bone morphology in 16 wk old female C57 mice following transient calf paralysis from a single injection of botulinum toxin A (BtA; 2U/100g body weight). In an acute study, we evaluated muscle and bone alterations at d 0, 3, 5 and 12 following transient calf paralysis. In a chronic study, following d 0 imaging, we assessed the recovery of these tissues following the maximum observed trabecular degradation (d 12) through d 84 post-paralysis. The time course and degree of recovery of muscle, trabecular and cortical bone varied substantially. Significant atrophy of lower limb muscle was evident by d 5 of paralysis, maximal at d 28 (−34.1 ± 0.9%) and partially recovered by d 84. Trabecular degradation within the proximal tibia metaphysis occurred more rapidly, with significant reduction in BV/TV by d 3, maximal loss at d 12 (−76.8 ± 2.9%) with only limited recovery by d 84 (−51.7 ± 5.1% vs. d 0). Significant cortical bone volume degradation at the tibia mid-diaphysis was first identified at d 12, was maximal at d 28 (−9.6 ± 1.2%), but completely recovered by d 84. The timing, magnitude and morphology of the observed bone erosion induced by transient muscle paralysis was consistent with a rapid recruitment and prolific activation of osteoclastic resorption. In a broader context, understanding how brief paralysis of a single muscle group can precipitate such rapid and profound bone resorption in an adjacent bone is likely to provide new insight into how normal muscle function modulates bone homeostasis.

Keywords

botulinum toxin; muscle paralysis; muscle atrophy; osteoclastogenesis; bone morphology

Corresponding author: Sandra L. Poliachik, Ph.D. 325 9th Avenue Box 359798 Seattle WA 98104 Phone: 206-897-5605 Fax: 206-897-5611.

Introduction

Although it is well recognized that impaired loading of the skeleton results in focal bone loss, the mechanisms underlying how disuse alters bone cell function remain unknown. The severity of bone loss due to immobilization can approach post-menopausal bone loss [1]. In spinal cord injury patients, for example, 40 to 50% of sub-lesion bone is lost within 2 to 8 years, depending upon assay and site [2,3]. It is therefore clear that some physiologic benefit is derived by skeletal loading achieved by muscular contraction [4].

A variety of small and large animal models have been used to explore disuse induced bone loss, which include but are not limited to tenetomy [5], limb casting [6], hindlimb suspension [7-11], and nerve disruption [12,13]. The complexity of local and systemic interactions underlying the skeletal response to disuse is reflected in the different processes by which bone morphology alterations are achieved in these models. For example, bone loss following hindlimb suspension arises due to decreased osteoblast function coupled with an increase in osteoclast function, but the more acute and profound bone loss observed following sciatic neurectomy arises primarily due to osteoclastic activation [14]. Importantly, one common finding in each of these models is that muscle atrophy is concomitant with the observed bone loss [8,9,13,15-18].

Recently, we developed a minimally invasive model of muscle dysfunction in which botulinum toxin A (BtA) is used to transiently paralyze murine hindlimb muscles. We observed a 54.3% reduction in trabecular BV/TV in the proximal tibia metaphysis and a 13.1% expansion of endocortical volume in the tibia mid-diaphysis compared to saline control mice within just 21 d [19]. A study that preceded ours had explored the effect of using BtA to paralyze the quadriceps of growing rats using measures of BMC and radiographic texture analysis, but only BMC was significantly diminished [20]. It is likely that the lower resolution assay (compared to high-resolution micro computed tomography (micro-CT)) and the growing animals contributed to the minimal response observed as compared to our initial study. Subsequent to our report, several studies (in both mice and rats) have reported varying degrees of bone degradation following BtA-induced muscle paralysis [21-23]. As might be expected, the quantity of bone loss following muscle paralysis has varied with dose of BtA, muscles paralyzed, evaluation time points, experimental design (e.g., comparison with contralateral bones or separate age matched animals) and resolution of the technique used to assess bone morphology changes.

In a recent preliminary study inducing only calf muscle paralysis, we observed trabecular bone degradation within the proximal tibia metaphysis that occurred within 5 days of paralysis [24]. Given the implications for understanding the cellular signaling driving this response, we hypothesized that transient muscle paralysis would cause rapid and extensive degradation of trabecular bone and that morphological evidence of that degradation would be apparent before 21 d. We therefore sought to define the time course of lower limb muscle atrophy and trabecular and cortical bone loss following transient paralysis of the calf muscles. We achieved this goal by using high-resolution serial micro-CT imaging to quantify alterations in lower limb soft tissue volume, trabecular bone morphology, and cortical bone morphology in an acute study (d 0 to d 12) and a chronic study (d 0 to d 84). We observed profound and significant trabecular bone loss within a week and found that this trabecular morphology was only partially restored by d 84, but that maximal cortical bone loss observed 28 d following induced muscle paralysis was completely recovered by d 84.

Materials and Methods

In vivo transient muscle paralysis model

Under isoflurane anesthesia on d 0 each mouse (16 wk old female C57B6) was weighed and given one IM injection of botulinum toxin A (Botox®, Allergan; 2 U/100g, 20 μl final volume) into the right calf muscle group (consisting of the gastrocnemius, soleus and plantaris muscles). For 4 d following the injection of BtA, each mouse received a subcutaneous injection of saline (800 μl). This procedure differs from our initial protocol [19], but mitigates whole body weight loss while retaining equivalent bone loss in the tibia (unpublished data). At 24 hr post injection, all mice were visually examined for calf paralysis by assessing whether the mice could extend their toes or demonstrate ankle plantarflexion during transient tail suspension. Mice were group housed with free ambulation and received food and water *ad libitum*. The University of Washington IACUC approved all procedures.

Experimental Design

Mice were weighed prior to each scan, with each set of scans lasted approximately 40 minutes. In the acute experiment (n = 10), *in vivo* imaging was performed on d 0, 3, and 5 following induction of paralysis, with a terminal scan on d 12. In the chronic study (n = 10), *in vivo* imaging was performed on d 0, 12, 28, and 56 following induction of muscle paralysis, with a final terminal scan on d 84. For each mouse, the d 0 data served as the baseline measurement.

Micro-CT Imaging and Analysis

Using a custom alignment device, all *in vivo* imaging occurred with the mice anesthetized with isoflurane. For each time point, an *in vivo* high-speed micro-CT scanner (Scanco vivaCT 40) was used to perform three scans. The first, at 21 μm voxel medium resolution, imaged from the proximal tibia epiphysis to the tibia-fibular junction. The second and third scans were both at high-resolution (10.5 μm voxel) and encompassed the proximal tibia metaphysis and tibia mid-diaphysis, respectively. The specific regions of analysis were: 1) distal edge of the tibia growth plate to the tibiafibula junction (approximately 12.5 mm) of the first scan for assessment of lower limb muscle volume, 2) a 0.8 mm thick section of the second scan, initiating at the distal edge of the proximal tibia metaphysis for trabecular bone morphology, and 3) a 1.0 mm thick section of the tibia mid-diaphysis (0.65 mm proximal to the tibia-fibula junction) for cortical bone morphology. Standard image analysis procedures were used to determine trabecular and cortical bone parameters, as we and others have done previously [10,15,19, 25-27]. User defined contour lines were drawn every 15 slices, and interim contour lines were morphed along the entire analysis region using vendor supplied algorithms. Lower limb muscle volume (M.V, mm^3) was assessed by drawing contour lines around the visible soft tissue and subtracting bone volume. In our preliminary validation studies, we found a significant linear correlation between alterations in micro-CT derived muscle volume at d 28 and diminished calf muscle wet weight compared to the contralateral calf following a single calf injection of BtA ($n = 12$, $R^2 = 0.77$, $p < 0.05$; unpublished data). In the proximal tibia metaphysis we determined trabecular fraction (BV/TV, %), trabecular number (Tb.N, 1/mm), trabecular thickness (Tb.Th, mm) and trabecular spacing (Tb.Sp, mm) for each mouse at each time point. The tibia middiaphysis cortical bone morphology outcomes included periosteal volume (Ps.V, mm^3), cortical volume (Ct.V, mm^3) endocortical volume (Ec.V, mm^3), and cortical thickness (Ct.Th, mm).

Statistics

For each outcome measure, a repeated measures factorial ANOVA was used to assess the statistical significance of the main effects and interactions of BtA treatment across observed time points. When ANOVA indicated significance, a Dunnett's multiple comparison was used

to evaluate significant treatment differences between the time point groups (p=0.05). Percent differences, unless specifically noted, were determined by comparison with d 0 data.

Results

Mice visibly demonstrated BtA-induced paralysis of the calf muscles within 24 hr (an inability to extend their toes or demonstrate ankle plantarflexion while transiently suspended). One mouse in the acute study did not show any signs of paralysis and was removed from the study. Body weight was not significantly diminished compared to d 0 at any time point in the acute study, with a maximum loss of 0.8% at d 5. In the chronic study, a significant decrease in body weight was observed at d 12 (−3.7% vs. d 0, $p < 0.05$). By d 28 this transient decrease was ameliorated (0.2% vs. d 0). All mice in both studies returned to normal ambulation within 3 wk, as determined by visual examination.

Acute Study

Lower limb muscle demonstrated significant atrophy within 5 d of induced calf paralysis (−13.2 ± 1.0%, $p < 0.001$ vs. d 0) with continued atrophy observed at d 12 (−28.3 ± 1.5%, $p < 0.001$ vs. d 0; Figure 1). Trabecular bone loss, as assessed by BV/TV, was significantly diminished by d 3 of the BtA injection (−25.5 ± 3.8%, $p < 0.05$; Figure 1). Continued profound erosion of trabecular bone was observed at d 5 (−51.5 ± 2.9%, $p < 0.001$) and d 12 (−76.8 ± 2.9%, $p < 0.001$). Descriptive parameters of trabecular morphology reflected this degradation, with Tb.Th significantly decreased at d 5 (−10.0 ± 2.1%, $p < 0.05$ vs. d 0), while Tb.N (−20.8 ± 4.2%, $p < 0.001$ vs. d 0) and Tb.Sp (+24.7 ± 5.9%, $p < 0.001$ vs. d 0) were significantly altered by d 12 (Table 1). At the tibia middiaphysis, a significant decrease in Ct.V occurred at d 12 (−7.4 ± 1.3%, $p < 0.05$), due to increased Ec.V (−8.9 ± 2.2%, $p = 0.12$; Figure 2) as Ps.V was unchanged. Significant Ct.Th degradation was also observed by d 12 (−7.5 ± 1.3%, $p < 0.05$; Table 1).

Chronic Study

No significant differences were noted in the muscle volume, trabecular bone or cortical bone outcome measures when comparing the last day of the acute study and first time point of the chronic study (i.e., 12 d following transient muscle paralysis). Maximum lower limb muscle atrophy was observed at d 28 following transient muscle paralysis (−34.1 ± 0.9%, $p < 0.001$ vs. d 0), with significant but incomplete recovery through d 84 (−12.0 ± 0.9%, $p < 0.001$ vs. d 0; + 33.6 ± 1.3% vs. d 28, $p < 0.001$; Figure 3). Maximum trabecular degradation, as assessed by BV/TV, was observed at d 12, with partial but statistically significant recovery observed by d 84 (−51.7 ± 5.1% vs. d 0, $p < 0.001$; +138.8 ± 29.1% vs. d 12, $p = 0.001$; Figure 3).

Recovery of Tb.N was not observed through d 84, while those trabeculae that remained at d 12 demonstrated progressively increasing Tb.Th that, at d 84, exceeded d 0 Tb.Th by +34.6 ± 3.2% ($p < 0.001$; Table 2). Tb.Sp did not demonstrate a statistically significant recovery vs. d 12 alterations. As in the acute study, Ps.V at the tibia middiaphysis was unchanged by transient muscle paralysis through the chronic study time course (Table 2). Diminished Ct.V was maximal at d 28 (−9.6 ± 1.2%, $p < 0.001$ vs. d 0), then progressively recovered such that the Ct.V at d 84 did not differ from d 0. Ct.V loss was achieved via increased Ec.V, which followed a temporally identical but inverse pattern of expansion (maximum at d 28; +11.8 ± 2.0%, $p = 0.001$ vs. d 0) and recovery such that the Ec.V at d 84 was equivalent to that of d 0 (Figure 4). As a result, Ct.Th was maximally diminished at d 28 (−11.7 ± 1.2%) but recovered completely by d 84 (Table 2).

Discussion

The coupling of acute and chronic time course data conclusively demonstrate rapid, time-dependent degradation of both tibia trabecular and cortical bone following transient paralysis of calf muscles. The time course and degree of recovery of muscle, trabecular bone and cortical bone outcome measures varied substantially. Significant atrophy of lower limb muscle was evident within 5 d of paralysis, was maximal at d 28 and recovered to 88% of the initial volume by d 84. Trabecular degradation was more rapid, with significant reduction in trabecular fraction by d 3, maximal loss at d 12, and a recovery to only 50% of initial values at d 84. Significant cortical bone degradation was first identified at d 12, was maximal at d 28 and completely recovered by d 84. At the least, these data confirm the essential role that normal muscle function plays in the homeostasis of an adjacent bone.

Before discussing the implications of these data, the primary limitations of the study should be considered. As previous studies have shown that trabecular bone volume ratio in the proximal tibia metaphysis of C57B6 female mice does change significantly through the age range observed this study (16 to 28 wk; [26]), we did not include intact control mice in our experimental design in order to minimize animal use. Unpublished data from our own preliminary studies suggests a similar lack of variation in cortical bone and lower limb muscle volume for this age range in this strain of female mice.

We split our study into separate acute and chronic components in part to limit radiation exposure for each mouse. Given the exposure parameters and number of scans, we estimate that the maximum cumulative exposure (in the chronic study) was half of the radiation exposure previously determined to not influence bone morphology in normal rats, and only minimally influence trabecular bone in mice [28,29]. Further, the rapid time course of trabecular bone degradation following transient muscle paralysis is distinct from the much slower degradation of trabecular bone due to much greater levels of radiation [30], yielding further confidence that radiation exposure itself was not a determining factor in the bone degradation induced by muscle paralysis.

We used serial *in vivo* imaging of lower hindlimb soft tissue atrophy as a surrogate for impaired function of the calf muscle group. Given the relative size of the calf muscle group compared to the lower hindlimb total tissue volume in the C57 female mouse, we observed a proportional decrease in soft tissue volume compared to our previous end point assays of wet muscle weight following BtA injection, but with the obvious advantages of using each mouse as an internal control and multiple sampling time points. A limitation of this approach, however, is that the observed atrophy of soft tissue in our study is likely to not coincide temporally with the degradation of calf muscle function (e.g., as assessed by determining force generation via muscle stimulation). Following transient muscle paralysis via BtA injection, muscle force generation has been shown to begin to degrade within a few hours [31], with maximum muscle force degradation occurring over a period of 3 to 10 days, depending on dose and age of the animal [32]. The duration and extent of paralysis in our study visually (i.e., via subjective assessment of gait function and activity) generally appeared to coincide with such a time course, although more direct measures will be implemented in future studies to clarify this aspect of the intervention.

The morphologic adaptation observed in the acute study is clearly suggestive of a process driven by osteoclastic resorption, as we have previously asserted [19], and further studies will clarify any potential contribution of diminished osteoblast activity to the observed response. As is clear in Figure 1, trabecular bone degradation was rapidly achieved via erosion of trabeculae, which requires a substantial shift in bone homeostasis towards bone resorption. Cortical bone loss was achieved by expansion of the endocortical surface, which also requires

an extensive increase in osteoclastic resorption. Finally, with our preliminary data indicating that bone loss in this model is completely mitigated by treatment with rhOPG [33], these observations build support for osteoclastogenesis as the initial bone cell response to transient muscle paralysis, while not yet ruling out a concurrent alteration in osteoblast function. The time required for osteoclastogenesis *in vivo* is 3 to 5 days [34], thus we infer that the signaling pathway responsible for driving osteoclast activation in our model is likely to be up-regulated (or down-regulated) within 24 hr of muscle paralysis.

One conclusion of the chronic study was that while acute cortical bone changes were eventually recovered, trabecular bone morphology was not, at least through 84 d post paralysis. In both compartments, morphologic adaptations reflect a transition from an osteoclastic dominated response to an osteoblastic dominated response. For the proximal tibia metaphysis, this shift occurred near d 12, while for cortical bone, the transition was near d 28 following BtA injection. As reflected in Figure 3, once trabeculae were perforated, the subsequent osteoblastic response was not able to reconnect trabecular morphology, but did result in the rebuilding of surviving trabeculae. In this context, the restoration of endocortical volume, presumably by coupled osteoblastic infilling of regions of resorption, is not surprising. Thus, the data of this morphologic study provide specific endpoints to clarify the cellular dynamics responsible for the observed degradation of trabecular and cortical bone via histomorphometry, while envelope specific signaling pathways responsible for coupling the osteoblastic response to an initial osteoclastic response (or the lack of coupling) may prove critical to understanding why cortical bone appeared to be more resilient to the challenge of transient muscle paralysis. As with human pathologies involving profound loss of trabecular bone, these data also emphasize that successful interventions in conditions in which profound osteoclastic activity is provoked must occur prior to structural degradation of trabeculae [35,36].

While this study has defined the acute and chronic morphologic consequences of transient muscle paralysis, it is of obvious interest to understand why a transient alteration in muscle function precipitates such a profound catabolic response in the adjacent bone. In our view, there are three reasonable pathways that are likely candidates for this process. First, there is little doubt that loss of calf muscle function precipitates diminished and altered locomotion in mice. The lessoning of total mechanical input (or altered strain distributions due to impaired gait) from transient paralysis, as induced in this study, is not known, but could be determined via a combination of *in vivo* strain gaging and activity assessment. Second, it has been suggested that muscle atrophy itself (via release of factors with direct action on bone cells) may induce the acute osteoclastic response noted here [37]. One challenge for this possibility is that it is not clear how a factor released outside of the bone compartment would result in such profound localized bone degradation rather than causing a systemic effect. Finally, muscle and bone share common innervation and vascularization. It is clear that neuronal signaling, endothelial signaling and smooth muscle cell signaling all have the ability to systemically and locally modulate bone cell function [38-42].

In this context, our initial study with this model used twice the total body dose of Botox which resulted in a transient, but statistically significant, decrease in body weight and a 17% loss of muscle mass in the contralateral quadriceps and calf muscles of mice exposed to Botox injection vs. saline control mice at 21 d [19]. Despite this systemic effect (which we avoided in the current study by reducing the total body dose of Botox), we did not observe any statistical differences in trabecular morphology of the proximal tibia (BV/TV, Tb.N, Tb.Th, Tb.Sp) or cortical morphology at the tibia mid-diaphysis (Ps.V, Ec.V, Ct.V) between contralateral tibiae from Botox or saline injected mice in that study. Further, preliminary data indicate that for a single 2 U/100 g Botox injection into the calf muscle group, there were no differences in contralateral calf wet muscle weight for Botox or saline injected groups at 21 d (unpublished data; n=8 per group). These data support the conclusion that at 21 d following induction of

muscle paralysis, contralateral bone morphology effects were not present. However, it is possible that a transient acute effect related to neuronal, endothelial or smooth muscle signaling is evident in this model and we intend to clarify this issue in future studies. Ultimately, we believe that site-specificity of the observed bone degradation in our model (or its lack thereof) will prove critical in attempting to isolate signaling pathways amongst such integrated and overlapping stimuli.

In summary, we note that transient paralysis of the calf muscle group, as achieved by a single dose of BtA, precipitates rapid and significant degradation of trabecular and cortical bone in the tibia of female C57 mice. The magnitude of acute trabecular bone loss observed in this study was surprising, yet the timing and extent is similar to pathological bone resorption that is induced by pharmacological doses of Vitamin D or PTH [43]. That such an apparently mild intervention, particularly in its transient nature, provoked such a profound response underscores the critical role of normal muscle function in maintaining bone homeostasis.

Acknowledgments

This work was supported, in part, by grants from NIAMS (AR45665) and The Christopher and Dana Reeve Foundation, and funding from the Sigvard T. Hansen, Jr. Endowed Chair.

References

1. Mazess RB, Whedon GD. Immobilization and bone. Calcif Tissue Int 1983;35:265–7. [PubMed: 6409385]
2. Eser P, Frotzler A, Zehnder Y, Wick L, Knecht H, Denoth J, Schiessl H. Relationship between the duration of paralysis and bone structure: a pQCT study of spinal cord injured individuals. Bone 2004;34:869–80. [PubMed: 15121019]
3. Shields RK, Dudley-Javoroski S, Boaldin KM, Corey TA, Fog DB, Ruen JM. Peripheral quantitative computed tomography: measurement sensitivity in persons with and without spinal cord injury. Arch Phys Med Rehabil 2006;87:1376–81. [PubMed: 17023249]
4. Frost HM. From Wolff's law to the Utah paradigm: insights about bone physiology and its clinical applications. Anat Rec 2001;262:398–419. [PubMed: 11275971]
5. Shaker JL, Fallon MD, Goldfarb S, Farber J, Attie MF. WR-2721 reduces bone loss after hindlimb tenotomy in rats. J Bone Miner Res 1989;4:885–90. [PubMed: 2558504]
6. Liu D, Zhao CQ, Li H, Jiang SD, Jiang LS, Dai LY. Effects of spinal cord injury and hindlimb immobilization on sublesional and supralesional bones in young growing rats. Bone 2008;43:119–25. [PubMed: 18482879]
7. Barou O, Valentin D, Vico L, Tirode C, Barbier A, Alexandre C, Lafage-Proust MH. High-resolution three-dimensional micro-computed tomography detects bone loss and changes in trabecular architecture early: comparison with DEXA and bone histomorphometry in a rat model of disuse osteoporosis. Invest Radiol 2002;37:40–6. [PubMed: 11753153]
8. Fisher JS, Hasser EM, Brown M. Effects of ovariectomy and hindlimb unloading on skeletal muscle. J Appl Physiol 1998;85:1316–21. [PubMed: 9760322]
9. Judex S, Garman R, Squire M, Busa B, Donahue LR, Rubin C. Genetically linked site-specificity of disuse osteoporosis. J Bone Miner Res 2004;19:607–13. [PubMed: 15005848]
10. Squire M, Brazin A, Keng Y, Judex S. Baseline bone morphometry and cellular activity modulate the degree of bone loss in the appendicular skeleton during disuse. Bone 2008;42:341–9. [PubMed: 17997144]
11. Weinreb M, Rodan GA, Thompson DD. Osteopenia in the immobilized rat hind limb is associated with increased bone resorption and decreased bone formation. Bone 1989;10:187–94. [PubMed: 2803854]
12. Kingery WS, Offley SC, Guo TZ, Davies MF, Clark JD, Jacobs CR. A substance P receptor (NK1) antagonist enhances the widespread osteoporotic effects of sciatic nerve section. Bone 2003;33:927–36. [PubMed: 14678852]

13. Zeng QQ, Jee WS, Bigornia AE, King JG Jr. D'Souza SM, Li XJ, Ma YF, Wechter WJ. Time responses of cancellous and cortical bones to sciatic neurectomy in growing female rats. Bone 1996;19:13–21. [PubMed: 8830982]

14. Marenzana M, De Souza RL, Chenu C. Blockade of beta-adrenergic signaling does not influence the bone mechano-adaptive response in mice. Bone 2007;41:206–15. [PubMed: 17543595]

15. Brouwers JE, Lambers FM, van Rietbergen B, Ito K, Huiskes R. Comparison of bone loss induced by ovariectomy and neurectomy in rats analyzed by in vivo micro-CT. J Orthop Res. 2009

16. Brown M, Foley A, Ferreria JA. Ovariectomy, hindlimb unweighting, and recovery effects on skeletal muscle in adult rats. Aviat Space Environ Med 2005;76:1012–8. [PubMed: 16315395]

17. Hutchinson KJ, Linderman JK, Basso DM. Skeletal muscle adaptations following spinal cord contusion injury in rat and the relationship to locomotor function: a time course study. J Neurotrauma 2001;18:1075–89. [PubMed: 11686494]

18. Picard S, Lapointe NP, Brown JP, Guertin PA. Histomorphometric and densitometric changes in the femora of spinal cord transected mice. Anat Rec (Hoboken) 2008;291:303–7. [PubMed: 18231968]

19. Warner SE, Sanford DA, Becker BA, Bain SD, Srinivasan S, Gross TS. Botox induced muscle paralysis rapidly degrades bone. Bone 2006;38:257–64. [PubMed: 16185943]

20. Chappard D, Chennebault A, Moreau M, Legrand E, Audran M, Basle MF. Texture analysis of X-ray radiographs is a more reliable descriptor of bone loss than mineral content in a rat model of localized disuse induced by the Clostridium botulinum toxin. Bone 2001;28:72–9. [PubMed: 11165945]

21. Blouin S, Gallois Y, Moreau MF, Basle MF, Chappard D. Disuse and orchidectomy have additional effects on bone loss in the aged male rat. Osteoporos Int 2007;18:85–92. [PubMed: 17019521]

22. Grimston SK, Silva MJ, Civitelli R. Bone loss after temporarily induced muscle paralysis by Botox is not fully recovered after 12 weeks. Ann N Y Acad Sci 2007;1116:444–60. [PubMed: 17584988]

23. Libouban H, Blouin S, Moreau MF, Basle MF, Audran M, Chappard D. Effects of risedronate in a rat model of osteopenia due to orchidectomy and disuse: densitometric, histomorphometric and microtomographic studies. Micron 2008;39:998–1007. [PubMed: 18023586]

24. Poliachik, SL.; B, S.; Srinivasan, S.; Ausk, BJ.; Threet, D.; Huber, P.; Gross, TS. Significant Trabecular Bone Degradation Occurs within Five Days of Muscle Paralysis. 30th Annual Meeting of American Society for Bone and Mineral Research; Montreal Canada. 2008;

25. Judex S, Garman R, Squire M, Donahue LR, Rubin C. Genetically based influences on the site-specific regulation of trabecular and cortical bone morphology. J Bone Miner Res 2004;19:600–6. [PubMed: 15005847]

26. Buie HR, Moore CP, Boyd SK. Postpubertal architectural developmental patterns differ between the L3 vertebra and proximal tibia in three inbred strains of mice. J Bone Miner Res 2008;23:2048–59. [PubMed: 18684086]

27. David V, Laroche N, Boudignon B, Lafage-Proust MH, Alexandre C, Ruegsegger P, Vico L. Noninvasive in vivo monitoring of bone architecture alterations in hindlimb-unloaded female rats using novel three-dimensional microcomputed tomography. J Bone Miner Res 2003;18:1622–31. [PubMed: 12968671]

28. Klinck RJ, Campbell GM, Boyd SK. Radiation effects on bone architecture in mice and rats resulting from in vivo micro-computed tomography scanning. Med Eng Phys 2008;30:888–95. [PubMed: 18249025]

29. Brouwers JE, van Rietbergen B, Huiskes R. No effects of in vivo micro-CT radiation on structural parameters and bone marrow cells in proximal tibia of wistar rats detected after eight weekly scans. J Orthop Res 2007;25:1325–32. [PubMed: 17568420]

30. Hamilton SA, Pecaut MJ, Gridley DS, Travis ND, Bandstra ER, Willey JS, Nelson GA, Bateman TA. A murine model for bone loss from therapeutic and space-relevant sources of radiation. J Appl Physiol 2006;101:789–93. [PubMed: 16741258]

31. Dimitrova DM, Shall MS, Goldberg SJ. Short-term effects of botulinum toxin on the lateral rectus muscle of the cat. Exp Brain Res 2002;147:449–55. [PubMed: 12444476]

32. Cichon JV Jr. McCaffrey TV, Litchy WJ, Knops JL. The effect of botulinum toxin type A injection on compound muscle action potential in an in vivo rat model. Laryngoscope 1995;105:144–8. [PubMed: 8544593]

33. Warner, SE.; S, S.; Kostenuik, PJ.; Gross, TS. 52nd Orthopaedic Research Society. Vol. 31. New Orleans: 2006. RANKL inhibition prevents the loss of bone volume and bone strength caused by Botox induced muscle paralysis; p. 189
34. Tran Van PT, Vignery A, Baron R. Cellular kinetics of the bone remodeling sequence in the rat. Anat Rec 1982;202:445–51. [PubMed: 7072987]
35. Ouyang X, Selby K, Lang P, Engelke K, Klifa C, Fan B, Zucconi F, Hottya G, Chen M, Majumdar S, Genant HK. High resolution magnetic resonance imaging of the calcaneus: age-related changes in trabecular structure and comparison with dual X-ray absorptiometry measurements. Calcif Tissue Int 1997;60:139–47. [PubMed: 9056161]
36. Slade JM, Bickel CS, Modlesky CM, Majumdar S, Dudley GA. Trabecular bone is more deteriorated in spinal cord injured versus estrogen-free postmenopausal women. Osteoporos Int 2005;16:263–72. [PubMed: 15338112]
37. Alzghoul MB, Gerrard D, Watkins BA, Hannon K. Ectopic expression of IGF-I and Shh by skeletal muscle inhibits disuse-mediated skeletal muscle atrophy and bone osteopenia in vivo. Faseb J 2004;18:221–3. [PubMed: 14597562]
38. Alam AS, Gallagher A, Shankar V, Ghatei MA, Datta HK, Huang CL, Moonga BS, Chambers TJ, Bloom SR, Zaidi M. Endothelin inhibits osteoclastic bone resorption by a direct effect on cell motility: implications for the vascular control of bone resorption. Endocrinology 1992;130:3617–24. [PubMed: 1597159]
39. Elefteriou F. Regulation of bone remodeling by the central and peripheral nervous system. Arch Biochem Biophys 2008;473:231–6. [PubMed: 18410742]
40. Goto T, Kido MA, Yamaza T, Tanaka T. Substance P and substance P receptors in bone and gingival tissues. Med Electron Microsc 2001;34:77–85. [PubMed: 11685656]
41. Niida S, Kondo T, Hiratsuka S, Hayashi S, Amizuka N, Noda T, Ikeda K, Shibuya M. VEGF receptor 1 signaling is essential for osteoclast development and bone marrow formation in colony-stimulating factor 1-deficient mice. Proc Natl Acad Sci U S A 2005;102:14016–21. [PubMed: 16172397]
42. Veillette CJ, von Schroeder HP. Endothelin-1 down-regulates the expression of vascular endothelial growth factor-A associated with osteoprogenitor proliferation and differentiation. Bone 2004;34:288–96. [PubMed: 14962807]
43. Morony S, Warmington K, Adamu S, Asuncion F, Geng Z, Grisanti M, Tan HL, Capparelli C, Starnes C, Weimann B, Dunstan CR, Kostenuik PJ. The inhibition of RANKL causes greater suppression of bone resorption and hypercalcemia compared with bisphosphonates in two models of humoral hypercalcemia of malignancy. Endocrinology 2005;146:3235–43. [PubMed: 15845617]

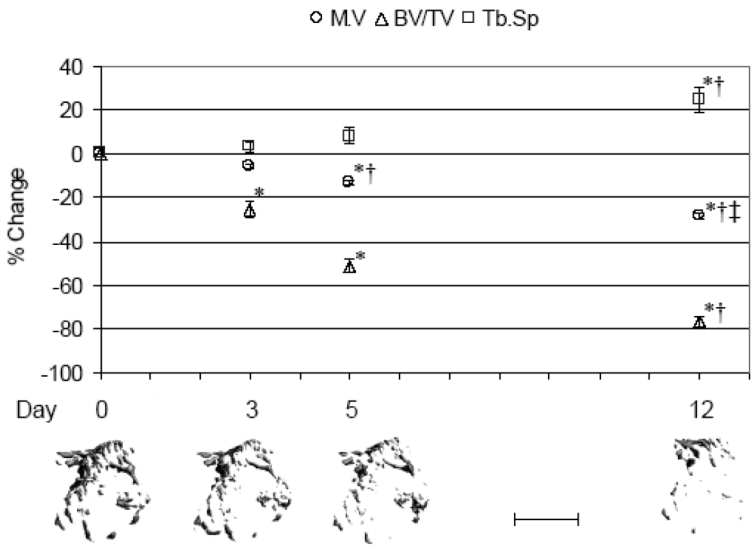

Fig 1.

Acute alterations in proximal tibia metaphysis trabecular morphology following BtA-induced transient muscle paralysis (mean ± S.E. percentage vs. d 0) at d 3, 5 and 12. Representative serial micro-CT images from the proximal tibia metaphysis of a single mouse visually demonstrate trabecular degradation observed within just a few days following induced paralysis. M.V: lower limb muscle volume, BV/TV: trabecular bone volume, Tb.Sp: trabecular spacing, with *: $p<0.05$ vs. d 0; †: $p< 0.05$ vs. d 3; ‡: $p< 0.05$ vs. d 5. Scale bar = 1 mm.

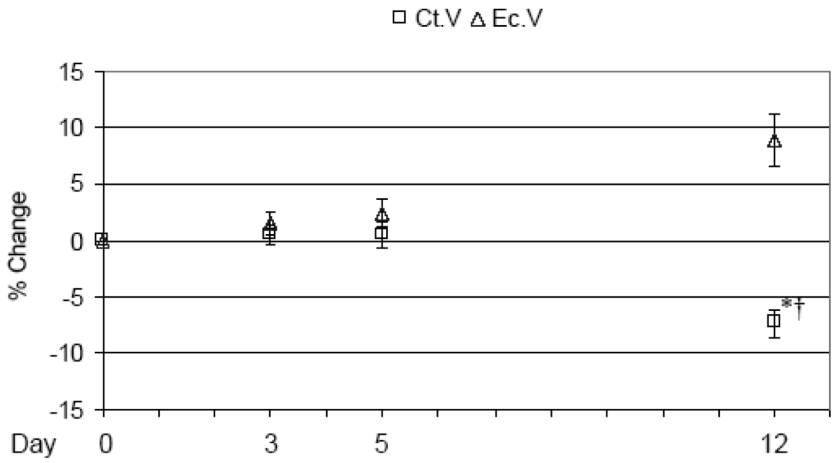

Fig 2.

Acute alterations in tibia mid-diaphysis morphology following BtA-induced transient muscle paralysis (mean percentage ± SE vs. d 0) at d 3, 5 and 12. Within this time period, only cortical bone (Ct.V) differences reached statistical significance. Ct.V: cortical bone volume, Ec.V: endocortical volume, with *: $p<0.05$; †: $p< 0.05$ vs. d 3.

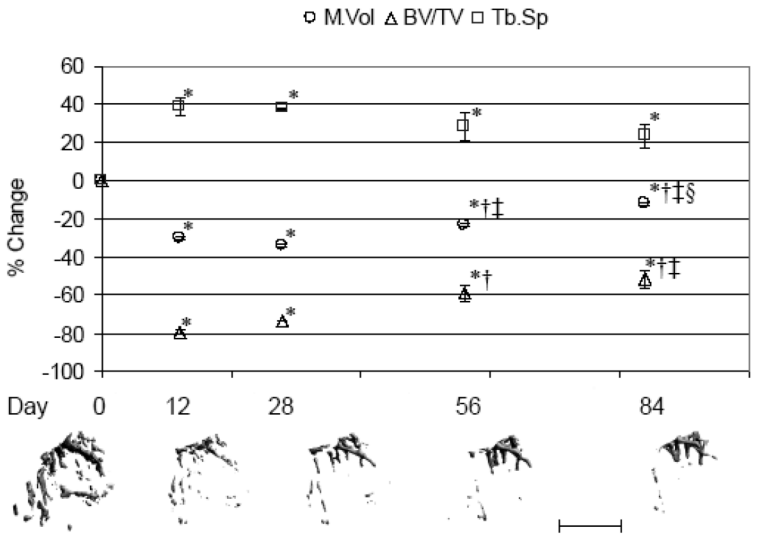

Fig 3.

Alterations in proximal tibia metaphysis trabecular morphology following BtA-induced transient muscle paralysis (mean percentage ± SE vs. d 0) at d 12, 28, 56 and 84. Representative serial micro-CT images from the proximal tibia metaphysis of a single mouse visually demonstrate profound degradation but only partial restoration of trabecular morphology by d 84. M. V: lower limb muscle volume, BV/TV: trabecular bone volume, Tb.Sp: trabecular spacing, with *: $p<0.05$ vs. d 0; †: $p< 0.05$ vs. d 12; ‡: $p< 0.05$ vs. d 28; §: $p < 0.05$ vs. d 56. Scale bar = 1 mm.

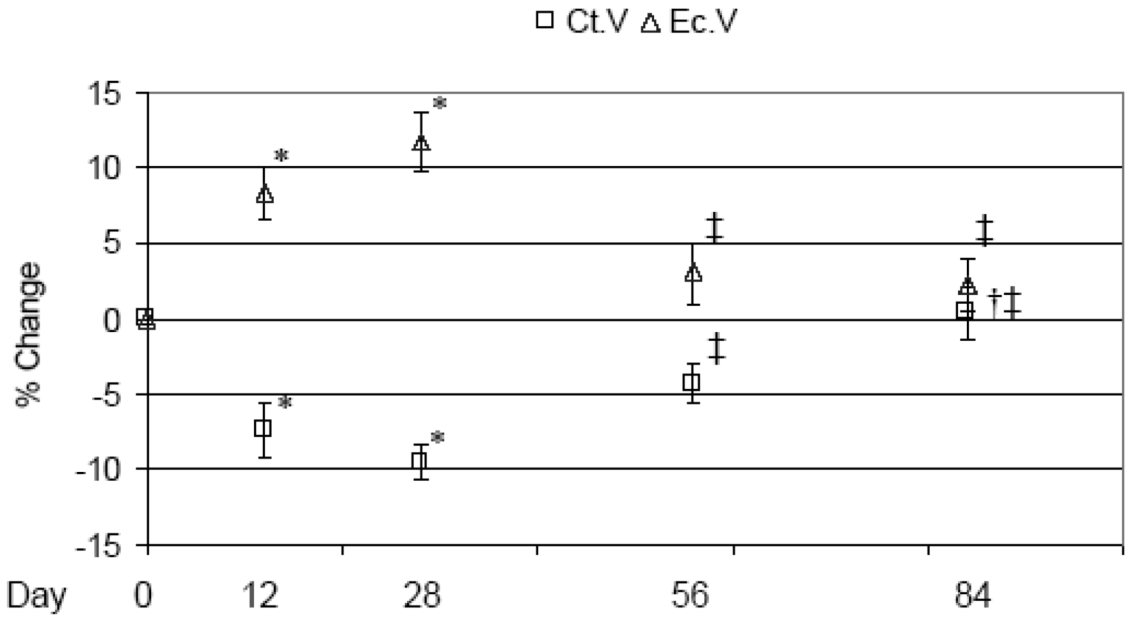

Fig 4.

Tissue changes in the tibia mid-diaphysis following BtA-induced transient muscle paralysis (mean percentage ± SE vs. d 0) at 12, 28, 56 and 84 d. The maximal degradation of cortical bone (Ct.V) was observed at 28 d due to expansion of the endocortical volume (Ec.V). By 84 d, however, this catabolic response was completely mitigated. Ct.V: cortical bone volume, Ec.V: endocortical volume, with *: $p<0.05$; †: $p< 0.001$ vs. d 0; ‡: $p<0.05$; § vs. d 28.

Table 1

Micro-CT outcome measures for the acute study.

	d 0	d 3	d 5	d 12
Lower limb muscle				
Muscle volume, M.V (mm^3)	312.58 ± 4.11	294.94 ± 3.59	271.38 ± 3.76^{ab}	223.58 ± 4.36^{abc}
Tibia proximal metaphysis				
Trabecular fraction, BV/TV (%)	0.038 ± 0.003	0.028 ± 0.003^{a}	0.019 ± 0.002^{a}	0.009 ± 0.001^{ab}
Trabecular number, Tb.N (#/mm)	2.822 ± 0.096	2.693 ± 0.078	2.527 ± 0.086	2.215 ± 0.083^{ab}
Trabecular thickness, Tb.Th (mm)	0.044 ± 0.001	0.043 ± 0.001	0.039 ± 0.001^{ab}	0.036 ± 0.001^{ab}
Trabecular spacing,Tb.Sp (mm)	0.376 ±0.010	0.388 ± 0.013	0.406 ± 0.014	0.466 ± 0.018^{ab}
Tibia mid-diaphysis				
Periosteal volume, Ps.V (mm^3)	1.039 ± 0.015	1.059 ± 0.014	1.053 ± 0.019	1.033 ± 0.019
Cortical volume, Ct.V (mm^3)	0.606 ± 0.006	0.611 ± 0.009	0.609 ± 0.010	0.561 ± 0.011^{ab}
Endocortical volume, Ec.V (mm^3)	0.437 ± 0.013	0.448 ± 0.010	0.444 ± 0.013	0.472 ± 0.017
Cortical thickness,Ct.Th (mm)	0.201 ± 0.003	0.200 ± 0.003	0.199 ± 0.003	0.186 ± 0.004^{a}

Significant differences noted by:

^{a} $p < 0.05$ vs. d 0

^{b} $p < 0.05$ vs. d 3

^{c} $p < 0.05$ vs. d 5.

Table 2

Micro-CT outcome measures for the chronic study.

	d 0	d 12	d 28	d 56	d 84
Lower limb muscle					
Muscle volume, M.V (mm^3)	316.66 ± 5.26	221.20 ± 5.19^{a}	208.83 ± 5.03^{a}	243.63 ± 5.57^{abc}	278.68 ± 5.67^{abcd}
Tibia proximal metaphysis					
Trabecular fraction, BV/TV (%)	0.031 ± 0.002	0.006 ± 0.000^{a}	0.008 ± 0.001^{a}	0.013 ± 0.002^{ab}	0.015 ± 0.002^{abc}
Trabecular number, Tb.N (#/mm)	2.894 ± 0.087	2.180 ± 0.063^{a}	2.209 ± 0.106^{a}	2.365 ± 0.142^{a}	2.356 ± 0.129^{a}
Trabecular thickness, Tb.Th (mm)	0.043 ± 0.001	0.035 ± 0.002^{a}	0.043 ± 0.002^{b}	0.052 ± 0.001^{abc}	0.057 ± 0.002^{abcd}
Trabecular spacing,Tb.Sp (mm)	0.350 ±0.010	0.483 ± 0.011^{a}	0.475 ± 0.020^{a}	0.446 ± 0.025^{a}	0.431 ± 0.026^{a}
Tibia mid-diaphysis					
Periosteal volume, Ps.V (mm^3)	1.053 ± 0.015	1.046 ± 0.014	1.049 ± 0.012	1.040 ± 0.013	1.064 ± 0.013
Cortical volume, Ct.V (mm^3)	0.596 ± 0.011	0.551 ± 0.009^{a}	0.538 ± 0.007^{a}	0.569 ± 0.006^{c}	0.597 ± 0.007^{bc}
Endocortical volume, Ec.V (mm^3)	0.457 ± 0.005	0.495 ± 0.009^{a}	0.510 ± 0.011^{a}	0.470 ± 0.011^{c}	0.467 ± 0.009^{c}
Cortical thickness, Ct.Th (mm)	0.194 ± 0.002	0.177 ± 0.002^{a}	0.171 ± 0.002^{a}	0.185 ± 0.002^{abc}	0.193 ± 0.002^{bc}

^{a} $p < 0.05$ vs. d 0

^{b} $p < 0.05$ vs. d 12

^{c} $p < 0.05$ vs. d 28

^{d} $p < 0.05$ vs. d 56.